Local structure in dilute nitrides probed by x-ray absorption spectroscopy

2004 J. Phys.: Condens. Matter 16 S3141

(http://iopscience.iop.org/0953-8984/16/31/010)

INSTITUTE OF PHYSICS PUBLISHING JOURNAL OF PHYSICS: CONDENSED MATTER

J. Phys.: Condens. Matter **16** (2004) S3141–S3150 PII: S0953-8984(04)75291-1

Local structure in dilute nitrides probed by x-ray absorption spectroscopy

G Ciatto[1] **and F Boscherini**[2,3]

[1] INFM, GILDA CRG, c/o ESRF, BP 220, 38043 Grenoble Cedex, France
[2] INFM and Department of Physics, University of Bologna, viale C Berti Pichat 6/2, 40127 Bologna, Italy

E-mail: federico.boscherini@bo.infm.it

Received 19 January 2004
Published 23 July 2004
Online at stacks.iop.org/JPhysCM/16/S3141
doi:10.1088/0953-8984/16/31/010

Abstract

We describe the use of x-ray absorption spectroscopy (XAS) with synchrotron radiation to study the local structure in dilute nitrides. After a brief description of the advantages of XAS to probe local atomic arrangements in semiconductor alloys we focus our attention on (InGa)(AsN). We discuss data which demonstrate that atomic ordering (in the form of an excess of In–N over Ga–N bonds) is present, but is significantly weaker than predicted; also, we show that the experimental values for the bond lengths are in agreement with recent models which take into account strain due to pseudomorphic growth.

1. X-ray absorption spectroscopy in the study of semiconductor alloys

A description and an understanding of the local atomic environment of semiconductor structures and alloys is of paramount important since it is the local (i.e. first and second atomic shell) interactions which determine, to a significant extent, the electronic and optical properties. In the field of semiconductor alloys the main advantages of x-ray absorption spectroscopy (XAS) are a fairly direct structural interpretation, atomic selectivity, a high precision in the determination of interatomic distances and the possibility to study, besides bulk or concentrated samples, monolayer-thin epilayers or dopants and implants (down to a concentration of $\sim 10^{18}$ atoms cm^{-3}). XAS was applied early on to semiconductor alloys. One important result which has stood the test of time is the demonstration that in bulk pseudobinary alloys such as InGaAs [1] and CdMnTe [2] significant local distortions occur. Other issues which can be studied are intermixing [3], atomic ordering [4] and strain-induced variations of bond lengths [5, 6].

[3] Author to whom any correspondence should be addressed.

In (InGa)(AsN) the relative disposition of cations and anions on their sublattices is not uniquely determined by the atomic concentration. In fact, in the zincblende structure each site of the anion (cation) sublattice can be occupied by In or Ga (As or N) without any limitation. Therefore, the question of the degree of atomic ordering, i.e. the relative number of each atomic bond as a function of composition, naturally arises. Specific examples of types of atomic ordering are the random case (relative number of each type of bond equal to the concentration) or short range ordering (SRO); in the relevant case of low N concentration SRO is exhibited, in the extreme cases, by a sample having only N–In or only N–Ga bonds. For (InGa)(AsN) it has been predicted that precisely this type of SRO exists, with a strong preference for In–N bonds over Ga–N ones [7]. Moreover, SRO has been predicted to cause a significant blue-shift of the bandgap and hence represent an intrinsic materials limitation. A similar effect has been previously predicted for (ZnMg)(SSe) [8]. Clearly, a quantification of SRO in (InGa)(AsN) is of crucial importance and XAS is the ideal experimental tool.

XAS [9] derives information on the local atomic structure from an analysis of the energy-dependent modulations of the x-ray-absorption cross-section which occur in condensed matter; these modulations appear at energies immediately above the threshold for photoelectric absorption (the 'absorption edge') in which the initial state is a deeply bound core orbital (most often 1s or 2p) and may extend from a few hundred to over one thousand electronvolts. The energy of the absorption edge is a characteristic of each element, so that it is possible to selectively probe the local structure around each element in a compound.

In order to measure an XAS spectrum with adequate signal-to-noise ratio and energy resolution a synchrotron radiation source is essential. Synchrotron radiation sources are relativistic electron accelerators which provide photon beams characterized by high brilliance and tunability over a wide energy range. Recently, a number of advanced 'third generation' synchrotron radiation sources have been constructed, one example of which is the European Synchrotron Radiation Facility (ESRF) in Grenoble, France. Third generation sources provide high quality photon beams which are essential to detect the changes in local structure induced by N incorporation in III–V semiconductor alloys, the topic of this paper.

Traditionally, the interpretation of XAS spectra has been divided into the analysis of the region within a few tens of electronvolts from the edge (XANES, x-ray absorption near edge structure, also known as NEXAFS, near edge x-ray absorption fine structure) and the analysis of the fine structure present sufficiently far from the edge, say 50 eV above the edge and beyond (EXAFS, extended x-ray absorption fine structure). Scattering theory provides a unifying picture of XAS in these two energy regions [10, 11]. Modulations in the x-ray absorption cross-section arise from a modification of the final state of the photo-excited electron due to the scattering by the atoms surrounding the excited one. In the absence of neighbouring atoms the final state would be an outgoing spherical wave. Instead, the presence of neighbouring atoms scatters this wave and, depending on the wavelength of the photoelectron and on the distance between excited and scattering atom, gives rise to an interference effect leading to an increase or a decrease of the x-ray-absorption cross-section. What distinguishes the two energy regions mentioned above is that far from the edge (EXAFS) single scattering of the photoelectron is usually dominant (only two atoms are involved in the process), while in the near edge region multiple scattering (more than two atoms involved) becomes increasingly more important. Each scattering path gives rise to a modulation of the x-ray-absorption cross-section which is a sinusoidal function of the photoelectron wavevector.

As an illustrative example, in figure 1(a) we show raw XAS data at the Ga K edge for bulk GaAs. In the top inset the relative modulations of the cross-section, or EXAFS function, are shown; the bottom inset reports the near edge structure (XANES). Figure 1(b) reports a Fourier transform of the EXAFS function, which provides an intuitive picture of local coordination:

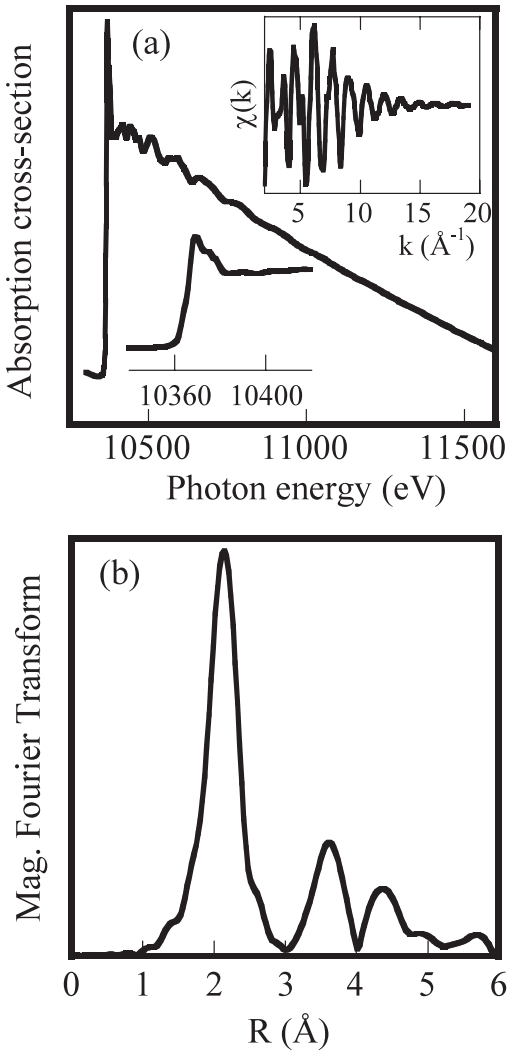

Figure 1. (a) Raw x-ray-absorption data at the Ga K edge for bulk GaAs; in the top inset we show the extracted EXAFS function, $\chi(k)$, as a function of photoelectron wavevector k, while in the bottom inset we report the near edge structure (XANES). (b) Magnitude of the Fourier transform for Ga K-edge EXAFS of GaAs as a function of interatomic distance R.

the first three peaks are related to the first three coordination shells around Ga, composed, in the present case, by As, Ga and As atoms in increasing order.

From the analysis of an EXAFS spectrum the following local structural parameters can be obtained: interatomic distances (R, typically ± 0.005 Å for the first shell), identity of neighbouring atoms and their coordination number (CN, typically $\pm 10\%$) and the variance of the Gaussian distance distribution function, also known as the 'Debye–Waller factor' (σ^2, typically $\pm 5 \times 10^{-4}$ Å^2). An analysis of the near edge spectrum provides information on the site symmetry of the absorbing atom (e.g. substitutional or interstitial) and on the composition of the first few coordination shells. The physical origin of the very local sensitivity of EXAFS is the limited lifetime of the core hole left by the photoabsorption process ($\sim 10^{-15}$ s) and short

Table 1. Sample characteristics.

Sample	Treatment	y (%)	x (%)	Max. ordering $y_{\mathrm{In-N}}$ (%)
633 V	As deposited	2.08	4.3	48
633 A1	Annealed 700 °C, 90 s	1.52	4.3	35
633 A2	Annealed 700 °C, 300 s	2.00	4.3	47
710 V	As deposited	0	3.6	0
711 V	As deposited	3.04	0	0
712 V	As deposited	3.35	3.8	88
712 A2	Annealed 700 °C, 300 s	3.27	3.8	86

mean free path (5–10 Å) of the photoelectron; the combination of these effects guarantees that atomic correlations at distances greater than ∼10 Å rarely contribute to an EXAFS spectrum.

2. A case study: (InGa)(AsN)

As mentioned above, the question of atomic ordering in (InGa)(AsN) is of importance both from a fundamental and from an applicative point of view. We have recently performed a detailed XAS study of ordering in this material, with the aim of quantifying the effect [12]; another report had provided indication that some ordering might be present, but no quantitative information had been provided [13]. In this paper we report a more complete account of our own work and discuss new data on bond lengths.

Measurements were performed on two series of 140 nm thick (InGa)(AsN) epilayers specifically designed to highlight the effects of SRO on the XAS data. The In and N concentrations (x and y, respectively) are similar ($x = 0.043$, $y \approx 0.02$ in the first series and $x = 0.038$, $y \approx 0.03$ in the second series; the exact N concentration for all samples is reported in table 1); since $x > y$, in the case of maximum In–N ordering each N atom would be coordinated solely by In atoms, while the relative In–N coordination number would be very high (about 40–50% for series I and almost 90% for series II). Samples were grown on a (001) GaAs substrate by gas-source molecular beam epitaxy using a radio-frequency plasma source, using a growth temperature of 400–430 °C; thermal annealing was performed in an RTA furnace under N_2 flow at 700 °C, for different times (90 and 300 s) [14]. The importance of studying SRO in annealed (InGa)(AsN) is related to three issues; firstly, annealing enhances the intensity of optical emission by removing non-radiative defects and is necessary in order to exploit these materials for applications; secondly, a blue-shift of the bandgap has been observed upon annealing [15, 16] and SRO may be at the origin of this phenomenon; lastly, annealing brings the system (close) to thermodynamic equilibrium, the condition which is most stable and which corresponds to the simulation. The In concentration was determined by Rutherford backscattering spectrometry, and the N concentration by combining (004) high resolution x-ray diffraction (HRXRD) and nuclear reaction analysis (NRA) measurements [17]; all epilayers were found by HRXRD reciprocal space mapping to be pseudomorphic to the GaAs substrate. For all (InGa)(AsN) samples analysed the strain was tensile, except for sample 633 A1 which has been grown virtually lattice matched to the GaAs substrate; the tensile-to-compressive transition occurs in fact, roughly, at concentrations for which $x = 3y$; for $x \leqslant 3y$ the strain is tensile. Trivially, for all GaAsN samples the strain was also tensile while for InGaAs sample 710 V it was compressive. NRA measurements, together with polarization dependent N K-edge XANES [18], guarantee that N is totally substitutional in the zincblende lattice. In table 1 we summarize the main sample characteristics; samples 710 and 711 serve as (InGa)As and Ga(AsN) references.

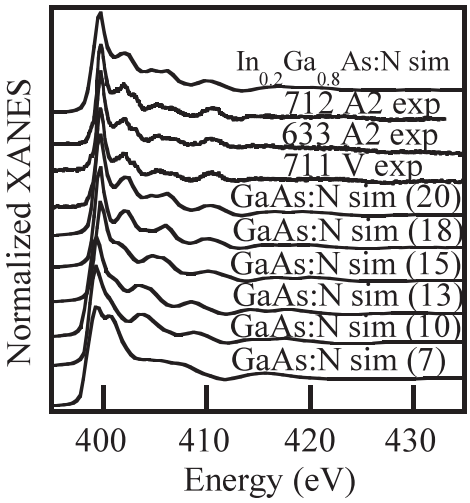

Figure 2. The bottom curves are simulations of the N K-edge XANES which show the evolution with increasing cluster size for an N atom embedded in GaAs (GaAs:N). The top curve is a simulation for an N atom embedded in $In_{0.2}Ga_{0.8}As$. Also shown are three experimental spectra for selected samples, characterized by different N and In concentrations and sample treatments.

N K-edge measurements were performed at the ELETTRA facility in Trieste, Italy (ALOISA beamline [19]), using a window-less single-element hyper-pure germanium detector to monitor the energy dependence of the N Kα fluorescence intensity. In K-edge measurements in an extended energy region were performed at the European Synchrotron Radiation Facility in Grenoble (BM8-GILDA CRG beamline), exploiting a sagittally focusing monochromator equipped with Si[311] crystals [20]. The In Kα fluorescence signal was monitored using a 13-element hyper-pure Ge detector. From the experimental point of view both the In-edge and the N-edge measurements are very demanding, and are possible only thanks to the properties of the third generation synchrotron radiation sources employed. At the N edge a very high photon brilliance is necessary since the N fluorescence yield is very small (10^{-3}); at the In edge a very good signal-to-noise ratio is essential to detect the weak contribution from N scattering atoms.

In figure 2 we report selected N K-edge near edge spectra (XANES) for one Ga(AsN) (711 V) and two (InGa)(AsN) samples (633 A2 and 712 A2). It is quite clear that all the experimental spectra are rather similar; even this qualitative observation hints at the fact that the local N environment is not very different in samples with or without In, even in samples in which maximum In–N ordering could give rise to a very In-rich environment.

The N-edge XANES spectra were interpreted on the basis of simulations in the full multiple-scattering approach using the program FEFF 8.0 [21], using self-consistency for the potential. The cluster for simulating Ga(AsN) was created by introducing an N impurity in the GaAs structure (GaAs:N) and relaxing the first and second shell distances through numerical minimization of the total energy [22], using a valence force field (VFF) potential [23] with appropriate force constants [24]. Relaxation beyond the second shell was found to have negligible effects on the simulations. The same procedure was adopted for an N impurity in InAs. These clusters consist of 20 atomic shells around the central N i.e. of 381 atoms; linear combinations of the simulated XANES spectra for GaAs:N and InAs:N were made in order to simulate the quaternary alloys with different In contents.

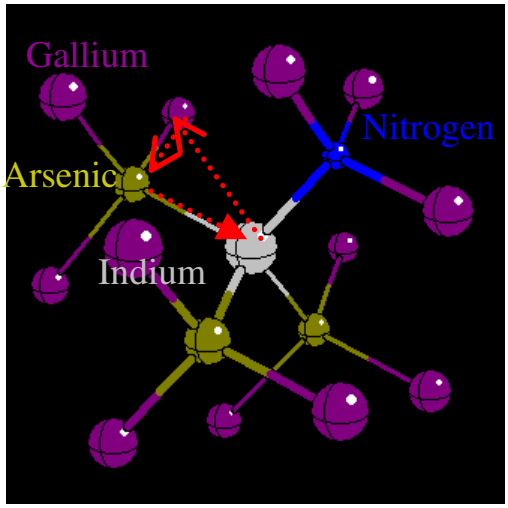

Figure 3. Local structure around an In atom in (InGa)(AsN). The dotted arrows depict the 'external triangle' multiple-scattering path.

(This figure is in colour only in the electronic version)

The bottom curves in figure 2 show the evolution of the simulated XANES with increasing number of coordination shells (from 7 to 20) around the photoexcited N atom included in the simulation cluster. It is evident that the simulation performed with fewer than 18 shells is inadequate, while there is little difference between the simulations performed with 18 or 20 shells. The 20-shell simulation reproduces quite well the three experimental spectra. The top curve in figure 2 reports a 20-shell simulation for an alloy with a 20% In coordination: significant differences in the lineshape and position exist relative to the experimental spectra. The conclusion from the N-edge XANES investigation is that the relative number of In atoms bonded to N is always less that 20%.

EXAFS oscillations at the In edge were extracted from the raw data with the AUTOBK code [25] using a spline with 15 free coefficients. Data analysis was performed by *ab initio* modelling of the XAFS signal using the FEFF 8.00 code [21]. The theoretical signals were calculated using (InGa)As and InN model clusters. Quantitative analysis was performed in the range $R = 1.6$–4.8 Å. The FEFFIT [26] program was used to extract the structural parameters. The data at the In K edge were fitted with a combination of In–As and In–N signals for the first shell and two distinct In–Ga contributions for the second shell; these two contributions are due to second shell Ga atoms linked to the central In via either As or N atoms and they occur at significantly different distances. A statistical analysis [12] shows that it is in fact necessary to include N-related paths in the fitting. A single parameter, $y_{\mathrm{In-N}}$, determines the relative weight of all the N-related structural signals; it is equal to the relative number of first shell N atoms around the average In atom ($y_{\mathrm{In-N}} = \{\text{In–N coordination number}\}/4$). Conservation of bonds dictates the relation between $y_{\mathrm{In-N}}$ and $x_{\mathrm{N-In}}$, the relative number of first shell In atoms around the average N atom: $yx_{\mathrm{N-In}} = xy_{\mathrm{In-N}}$.

The third shell is taken into account by a single In–As path; only one multiple-scattering signal, due to the triangular atomic arrangement involving the central In, a second shell Ga and a first shell As atom, was found to have a significant amplitude and was included. This path is illustrated in figure 3 as the red dashed line. The distance fitting parameters were the In–As first shell, two In–Ga second shell and one In–As third shell distances. Due to the relative

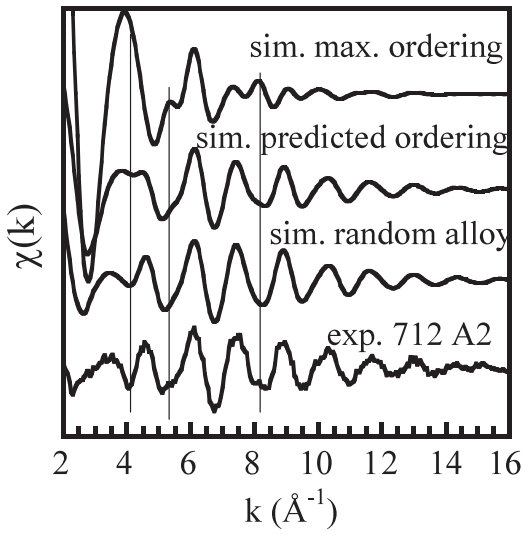

Figure 4. Experimental In K-edge EXAFS for sample 712 A2, and simulations for the cases of random, predicted and maximum ordering; the straight lines indicate the positions of spectral features discussed in the text.

Table 2. Values of interatomic distances and Debye–Waller factors; all errors are 1σ values.

Sample	$R_{\mathrm{In-As}}$ (Å)	$R_{\mathrm{In-(N)-Ga}}$ (Å)	$R_{\mathrm{In-(As)-Ga}}$ (Å)	$\sigma^2_{1\mathrm{st}}$ (10^{-3} Å^2)	$\sigma^2_{2\mathrm{nd}}$ (10^{-3} Å^2)
633 V	2.580 ± 0.004	—	4.067 ± 0.008	3.9 ± 0.1	9 ± 2
633 A1	2.583 ± 0.004	3.59 ± 0.05	4.076 ± 0.006	2.5 ± 0.2	7 ± 2
633 A2	2.579 ± 0.006	3.53 ± 0.07	4.056 ± 0.011	3.9 ± 0.4	11 ± 1
710 V	2.583 ± 0.006	—	4.079 ± 0.017	4.0 ± 0.2	12 ± 2
712 V	2.587 ± 0.004	3.53 ± 0.06	4.085 ± 0.009	3.6 ± 0.3	14 ± 1
712 A2	2.595 ± 0.004	3.62 ± 0.05	4.089 ± 0.024	3.6 ± 0.4	13 ± 2
InAs	2.623	—	$R_{\mathrm{In-(As)-In}} = 4.284$		

weakness of the signal it was found to be necessary to fix the In–N distance; this bond length was fixed to the value predicted by a VFF model [28], correcting for the effect of strain [27] (see equation (2) below). Four Debye–Waller factors were used for the three single-scattering and one multiple-scattering signals. Finally, for all shells a common non-structural parameter was the threshold energy shift (in the range 7–9 eV); the many-body amplitude reduction factor was fixed to the value found from an analysis of an InAs powder sample. Values of first and second shell interatomic distances and Debye–Waller factors are reported in table 2.

In figure 4 we show, from bottom to top, the extracted EXAFS oscillations for the sample which will be shown in the following to exhibit the greatest degree of In–N ordering (712 A2), and three simulations for a random atomic arrangement and degrees of ordering equal to that predicted by Kim and Zunger [7] and to the maximum possible ordering compatible with In and N concentrations. A qualitative discussion of these data is instructive. The simulation for maximum ordering is clearly different from the experimental spectrum: it has an envelope which is a monotonically decreasing function of the wavevector k and a large positive oscillation at $k \sim 4$ Å^{-1}, a position at which the experimental data has a small negative oscillation. The simulation for the predicted ordering is more similar to the data but significant differences,

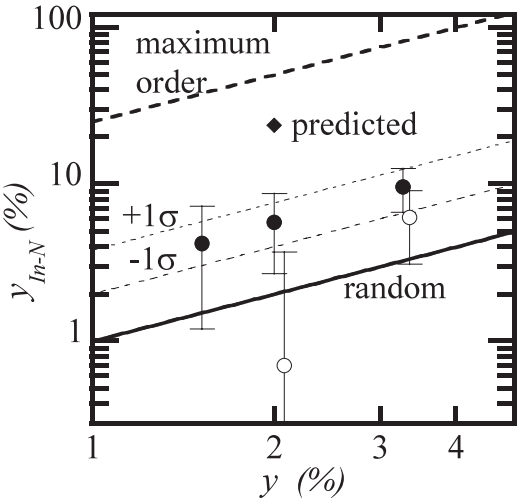

Figure 5. Relative In–N coordination number versus concentration. Open circles, as-deposited samples; full circles, annealed samples; diamond, prediction by Kim and Zunger [7]; top dashed line, maximum ordering; thin dashed lines, linear fits to annealed samples with $\pm 1\sigma$ slope; continuous line, random ordering.

again especially evident at $k \sim 4$ Å^{-1}, exist. However, the experimental spectrum is not identical to the simulation for random ordering; in fact at $k \sim 5.5$ and $k \sim 8.2$ Å^{-1} the experimental spectrum exhibits small positive peaks which suggest the presence of atomic ordering since they appear in the corresponding simulation; in particular, the second of these two peaks appears in the experimental spectrum only upon annealing as consistent with an increased degree of ordering.

The results of the fitting of the In-edge EXAFS put on a quantitative basis the indications of the N-edge XANES and of the inspection of figure 4. In figure 5 we report values of $y_{\mathrm{In–N}}$ as a function of the N concentration y; the three filled circles are relative to the annealed samples, while the empty circles refer to as-deposited samples; the diamond shows the prediction by Kim and Zunger [7], the top dashed line indicates the expected behaviour for maximum ordering and the continuous line that for random ordering ($y_{\mathrm{In–N}} = y$). We have fitted the experimental points for the annealed samples with a straight line with zero intercept: $y_{\mathrm{In–N}} = my$, the value of the slope m indicating the degree of ordering. We found $m = 2.9$, and $\sigma_m = 0.9$, using the 1σ error on $y_{\mathrm{In–N}}$, as big as it is, to determine σ_m; therefore, the annealed samples deviate from the random ordering case within 2σ. In figure 5 the thin dashed lines indicate a slope equal to the best value $\pm 1\sigma$. While this demonstrates that atomic ordering is present in annealed samples, the effect is significantly less than predicted by Kim and Zunger (diamond in figure 5).

In table 2 we report the values of In–As first shell and In–Ga second shell interatomic distances. We will discuss them in that order. All In–As bond lengths are significantly shorter than the value found in the reference crystal of bulk, pure, InAs. This contraction can be understood as originating from a combination of two effects [5, 27]: the effect, at a local scale, of the change in lattice parameter due to alloying and the variation induced by the tetragonal deformation of the unit cell due to pseudomorphic growth.

We use the work of Cai and Thorpe (CT) [28] to estimate the alloying effect. CT have developed an analytic model which is in quantitative agreement with XAS data on unstrained,

bulk, semiconductor alloys. Adopting a valence force field [23] potential to describe local structural distortions, CT introduce a rigidity parameter a^{**} which describes the resistance of a given lattice to a radial expansion: $a^{**} = 1$ indicates the lattice is floppy and each bond is fixed at its 'natural' length (Pauling's limit) while $a^{**} = 0$ indicates the lattice is perfectly rigid and that bond lengths obey the virtual crystal approximation; quite covalent semiconductors such as III–Vs are characterized by smaller values of a^{**} while more ionic systems such as II–VIs exhibit higher values; nevertheless, in all cases the floppy limit gives a better approximation than the rigid one. The main approximation of this model is that differences in bond force constants are neglected, an average value being adopted. Following CT, the In–As bond length in $In_xGa_{1-x}As_{1-y}N_y$ is given by

$$\begin{aligned} R_{\mathrm{In-As}} &= R_{\mathrm{V}} + a^{**}[(1-x)\Delta_{\mathrm{InGa}} + y\Delta_{\mathrm{As-N}}] \\ R_{\mathrm{V}} &= (1-x)(1-y)R^0_{\mathrm{Ga-As}} + (1-x)yR^0_{\mathrm{Ga-N}} + x(1-y)R^0_{\mathrm{In-As}} + xyR^0_{\mathrm{In-N}} \end{aligned} \tag{1}$$

where R_{V} is the bond length in the virtual crystal approximation, $\Delta_{\mathrm{A-B}}$ is the difference of the atomic radii of atoms A and B and R^0_{XY} is the bond length in the binary compound XY (equal to the sum of the atomic radii).

To take into account the effect of strain we use a method which was very successful in the case of (InGa)As epilayers deposited on InP(001) [5, 27]. The method projects to the local scale the tetragonal distortion of the unit cell; its prediction for the strain-induced variation of bond lengths is

$$\delta R^{\mathrm{st}} = \frac{a_{\mathrm{f}}}{2\sqrt{3}}\left[1 - \frac{C_{12}}{C_{11}}\right]\frac{a_{\parallel} - a_{\mathrm{f}}}{a_{\mathrm{f}}} \tag{2}$$

where a_{f} and $a_{\parallel}$ are the free and in-plane lattice parameters, respectively, and C_{12} and C_{11} are the elastic constants. If $a_{\mathrm{f}} > a_{\parallel}$ (compressive strain), δR^{st} is negative, and vice versa. Using CT's model to calculate the value of the In–As bond length in a hypothetical (InGa)(AsN) unstrained alloy and summing with this the strain-induced variation we predict values of 2.586 Å for the N-free 710 V sample and 2.589 Å for all the others. In the case of sample 712 A2, for example, the CT model gives a value of 2.585 Å for the In–As bond length, the strain-induced variation is $+3.7 \times 10^{-3}$ Å and therefore the final value is 2.589 Å for the sum. These values are in very good agreement with the experimental ones.

In table 2 we also report the values of the second shell In–Ga distances. While in the parent InAs compound only one second shell distance exists, two separate contributions are detected in the samples, with a significant ∼0.5 Å splitting: one due to Ga linked via As, the other due to Ga linked via N. The value of this second shell splitting is in agreement with CT's model. A more detailed study of the second shell distances, which for a strained film are different in and out of the growth plane, would involve polarization dependent measurements [29].

3. Conclusion

XAS is powerful tool to study local structure in semiconductor alloys. With the use of third generation synchrotron radiation facilities the high quality data needed to study the subtle changes in local structure induced by N incorporation in III–V semiconductors can be obtained. We have reported data on (InGa)(AsN) which show that for annealed samples atomic ordering (more In–N bonds than for the random case) is present, but is significantly smaller than predicted; the measured values of interatomic distances are in agreement with recent models which take into account alloying and strain effects.

Acknowledgments

We acknowledge collaboration and are grateful for stimulating discussions with H Mariette, L Grenouillet, M Capizzi, A Polimeni, F D'Acapito, D De Salvador and S Mobilio. This work was supported in part by a COFIN-2001 grant from the Italian Ministry of Research, and by a PURS grant from the Synchrotron Radiation Committee of Istituto Nazionale per la Fisica della Materia (INFM), Italy.

References

[1] Mikkelsen J C Jr and Boyce J B 1982 *Phys. Rev. Lett.* **49** 1412
Mikkelsen J C Jr and Boyce J B 1983 *Phys. Rev.* B **28** 7130
[2] Balzarotti A, Czyzyk M, Kisiel A, Motta N, Podgorny M and Zimnal-Starnawska M 1984 *Phys. Rev.* B **30** 2295
[3] Boscherini F, Capellini G, DiGaspare L, Motta N, Rosei F and Mobilio S 2000 *Appl. Phys. Lett.* **76** 682
[4] Pascarelli S, Boscherini F, Mobilio S and Evangelisti F 1992 *Phys. Rev.* B **45** 1650
[5] Romanato F, De Salvador D, Berti M, Drigo A, Natali M, Tormen M, Rossetto G, Pascarelli S, Boscherini F, Lamberti C and Mobilio S 1998 *Phys. Rev.* B **57** 14619
[6] Lamberti C, Groppo E, Prestipino C, Casassa S, Ferrari A M, Pisani C, Giovanardi C, Luches P, Valeri S and Boscherini F 2003 *Phys. Rev. Lett.* **91** 046101
[7] Kim K and Zunger A 2001 *Phys. Rev. Lett.* **86** 2609
[8] Saitta A M, de Gironcoli S and Baroni S 1998 *Phys. Rev. Lett.* **80** 4939
[9] Koningsberger D C and Prins R (ed) 1988 *X-ray Absorption: Principles, Applications, Techniques of EXAFS, SEXAFS and XANES* (New York: Wiley)
[10] Natoli C R and Benfatto M 1986 *J. Physique Coll.* **47** C8
[11] For a recent theoretical review see: Rehr J J and Albers R C 2000 *Rev. Mod. Phys.* **72** 621
[12] Ciatto G, D'Acapito F, Grenouillet L, Mariette H, De Salvador D, Bisognin G, Carboni R, Floreano L, Gotter R, Mobilio S and Boscherini F 2003 *Phys. Rev.* B **68** 161201(R)
[13] Lordi V, Gambin V, Friederich S, Funk T, Takizawa T, Uno K and Harris J S 2003 *Phys. Rev. Lett.* **90** 145505
[14] Grenouillet L, Bru-Chevallier C, Guillot G, Gilet P, Ballet P, Duvaut P, Rolland G and Million A 2002 *J. Appl. Phys.* **91** 5902
[15] Spruytte S G, Coldren C W, Harris J S, Wampler W, Krispin P K, Ploog K and Larson M C 2001 *J. Appl. Phys.* **89** 4401
[16] Kudrawiec R, Sek G, Misiewicz J, Gollub D and Forchel A 2003 *Appl. Phys. Lett.* **83** 2772
[17] Bisognin G, DeSalvador D, Mattevi C, Berti M, Drigo A V, Ciatto G, Grenouillet L, Duvaut P, Gilet P and Mariette H 2004 *J. Appl. Phys.* **95** 48
[18] Ciatto G, Boscherini F, D'Acapito F, De Salvador D, Batchelor D, Carboni R, Grenouillet L, Mariette H and Mobilio S 2004 *Phys. Scr.* at press
[19] Floreano L, Naletto G, Cvetko D, Gotter R, Malvezzi M, Marassi L, Morgante A, Santaniello A, Verdini A and Tommasini F 1999 *Rev. Sci. Instrum.* **70** 3855
[20] Pascarelli S, Boscherini F, D'Acapito F, Hrdy J, Meneghini C and Mobilio S 1996 *J. Synchrotron Radiat.* **3** 147
[21] Ankudinov A L, Ravel B, Rehr J J and Conradson S D 1998 *Phys. Rev.* B **58** 7565
[22] Martins J and Zunger A 1984 *Phys. Rev.* B **30** 6217
[23] Keating P N 1966 *Phys. Rev.* B **145** 637
[24] Martin R M 1970 *Phys. Rev.* B **1** 4005
Wright A F 1997 *J. Appl. Phys.* **82** 2833
[25] Newville M, Livins P, Yacoby Y, Rehr J J and Stern E A 1993 *Phys. Rev.* B **47** 14126
[26] Newville M, Ravel B, Haskel D, Rehr J J, Stern E A and Yacoby Y 1995 *Physica* B **208/209** 154
[27] Tormen M, DeSalvador D, Natali M, Drigo A, Romanato F, Boscherini F and Mobilio S 1999 *J. Appl. Phys.* **86** 2533
[28] Cai Y and Thorpe M F 1992 *Phys. Rev.* B **46** 15872
Cai Y and Thorpe M F 1992 *Phys. Rev.* B **46** 15879
[29] Tormen M, De Salvador D, Drigo A V, Romanato F, Boscherini F and Mobilio S 2001 *Phys. Rev.* B **63** 115326